J|A|C|S COMMUNICATIONS

Published on Web 08/17/2009

Expression of Sensitized Eu^{3+} Luminescence at a Multivalent Interface

Shu-Han Hsu,[†,‡] M. Deniz Yilmaz,[†] Christian Blum,[§] Vinod Subramaniam,[§] David N. Reinhoudt,[†,‡] Aldrik H. Velders,[*,‡] and Jurriaan Huskens[*,†]

Molecular Nanofabrication Group, Laboratory of Supramolecular Chemistry and Technology, Biophysical Engineering Group, MESA+ Institute for Nanotechnology, University of Twente, P.O. Box 217, 7500 AE Enschede, The Netherlands

Received June 10, 2009; E-mail: j.huskens@utwente.nl; a.h.velders@utwente.nl

Self-assembly provides a unique paradigm to obtain complex and functional molecular architectures in a spontaneous process from small building blocks.[1] Self-assembly at surfaces is particularly rewarding since the inherent immobilization allows characterization by single molecule techniques[2] and potential embedding in a device structure. It has only been recently recognized that surfaces, in particular those functionalized with molecular recognition units, the so-called molecular printboards, offer additional benefits regarding control over molecular orientation, footprint, stability of binding, and suppression of nonspecific interactions.[3,4] These properties are given by the fact that molecules and complexes can be bound to such surfaces via multivalent interactions, which are governed by the principle of effective molarity.[4] When complexity is increased,[5] here when going from one to more interaction motifs, new emerging properties can be expected. It has been shown before that the use of building blocks with orthogonal interaction motifs that self-assemble on molecular printboards can lead to the selective formation of one type of complex (from a large number of potential complexes) consisting of more than two different building blocks[6] and control over supramolecular aggregation of receptor-functionalized vesicles.[7] Here we show, for the first time, the spontaneous formation of such a complex that signals its own correct assembly, by expressing sensitized lanthanide luminescence. The focus is on addressing the exact stoichiometry of the complex and its signaling properties.

The trivalent cations of several lanthanides and their complexes with organic ligands are known to exhibit characteristic emission line shapes, relatively long luminescence lifetimes, and a strong sensitivity toward quenching by high frequency, e.g., O−H, oscillators.[8] Because of their sharp, narrow absorption peaks and low absorption coefficients, lanthanide ions are usually excited via energy transfer from an excited organic chromophore (the antenna or sensitizer) that has a much higher absorption coefficient.[9] The energy transfer process is strongly distance dependent and limits the practical lanthanide-antenna distance to <5 Å.[10] Photophysical properties of lanthanide complexes in solution have been extensively studied. In a supramolecular example, an EDTA-based ligand with β-cyclodextrin (β-CD) binding sites showed sensitized Eu^{3+} emission by noncovalent capture of an organic sensitizer.[11] The immobilization and photophysical properties of lanthanide complexes on surfaces have not been investigated, except for some recent examples in which a Eu^{3+} complex was bound to a particle surface,[12] especially for sensor applications.[13]

Here, we employ antenna-sensitized Eu^{3+} luminescence based on host−guest interactions on the molecular printboard, which allows qualitative and quantitative studies of the complexation of four different building blocks (Figure 1): an EDTA-based ligand for binding a Eu^{3+} ion and the receptor surface, the Eu^{3+} ion, a naphthalene-based antenna molecule with receptor-binding moieties and with a carboxylate group for coordination to the Eu^{3+} ion, and a β-CD monolayer which functions as the receptor surface. The EDTA ligand and the antenna molecule are equipped with adamantyl groups (Ad) for noncovalent anchoring to the β-CD monolayer. The β-CD monolayer is used to immobilize both the sensitizer and the Eu^{3+} complex, thus enforcing the close proximity of the molecules and facilitating sensitized lanthanide luminescence owing to efficient energy transfer (Figure 1b).

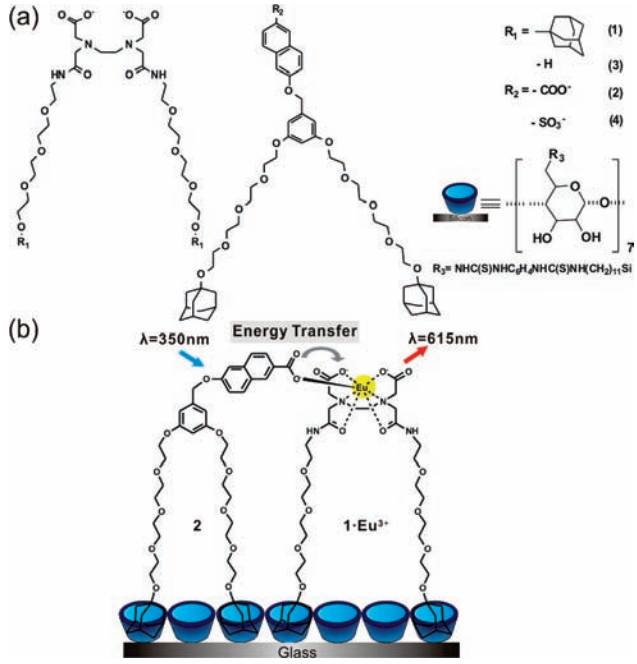

Figure 1. (a) EDTA-based ligands with (**1**) and without (**3**) adamantyl (Ad) moieties, and carboxylate- (**2**) or sulfonate- (**4**) modified naphthalene derivatives with Ad groups. (b) Molecular structure of the target complex on a β-CD SAM schematically showing sensitized Eu^{3+} luminescence.

Microcontact printing (μCP) onto β-CD monolayers, resulting in host−guest complex formation,[14] was used to generate surface patterns of complex on the receptor surface. Two methods were applied to immobilize the complex onto the surface (Scheme 1): (i) the surfaces were patterned by printing an equimolar ratio of **1**·Eu^{3+} and **2** onto the β-CD SAM ($\mathbf{i}_a$), followed by backfilling the nonprinted area with **1**·Eu^{3+}, which was used as an internal reference ($\mathbf{i}_b$); (ii) the surfaces were patterned by printing different ratios of **1** and **2** ($\mathbf{ii}_a$), followed by solution immersion in aqueous $EuCl_3$ ($\mathbf{ii}_b$). The solution immersion steps ($\mathbf{i}_b$ and $\mathbf{ii}_b$) were performed

[†] Molecular Nanofabrication Group.
[‡] Laboratory of Supramolecular Chemistry and Technology.
[§] Biophysical Engineering Group.

10.1021/ja904747p CCC: $40.75

Scheme 1. Schematic Representation of Two Immobilization Procedures (**i** and **ii**) of the Ad Ligands **1** and **2** without ($\mathbf{i}_a$, $\mathbf{ii}_a$) or with ($\mathbf{i}_b$, $\mathbf{ii}_b$) a Solution Step for Backfilling with **1**·Eu^{3+} in the Nonprinted Area ($\mathbf{i}_b$) or Complexation of **1** with Eu^{3+} ($\mathbf{ii}_b$)

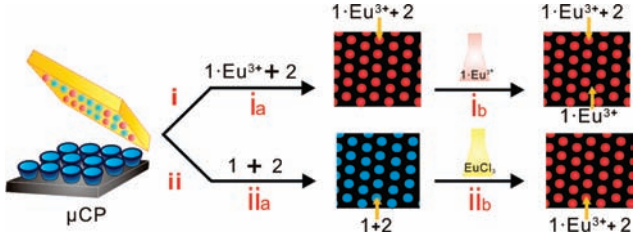

in the absence of β-CD in solution to prevent exchange of **2** by **1**·Eu^{3+} ($\mathbf{i}_b$) and desorption of **1** and **2** ($\mathbf{ii}_b$).[10]

As an initial indication for energy transfer at the molecular printboard patterned using method **i**, red emission measured using filter **R**14 only appeared in the areas where both **1**·Eu^{3+} and **2** are present (Figure 2), in contrast to the background which only

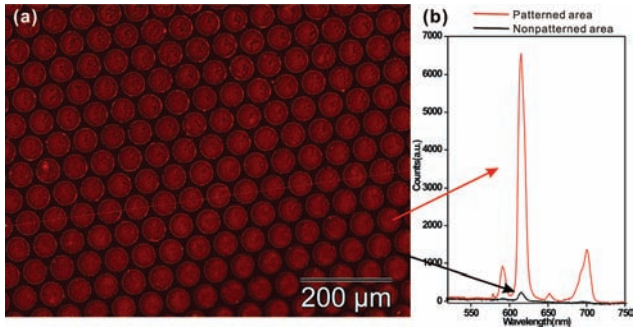

Figure 2. (a) Fluorescence microscopy image (left, using filter **R**[14]) of 50 μm dots on a β-CD monolayer obtained by μCP of an equimolar ratio of **1**·Eu^{3+} and **2** for 30 min (step $\mathbf{i}_a$) and subsequent incubation in a solution with **1**·Eu^{3+} for 30 min (step $\mathbf{i}_b$). (b) Local emission spectra from the patterned and nonpatterned areas, both illustrating the enhanced Eu^{3+} emission in the patterned areas.

contained **1**·Eu^{3+}. This demonstrates qualitatively the occurrence of sensitized Eu^{3+} luminescence. In contrast, when using **4**, a naphthalene moiety bearing a sulfonate group instead of the carboxylate in **2**, no sensitized Eu^{3+} luminescence was observed. Since the sulfonate group is not basic enough to bind a lanthanide ion, this shows that direct coordination of the carboxylate of **2** to the Eu^{3+} center is involved to obtain efficient energy transfer. A similar observation was made in solution.[11] Moreover, when an EDTA-based complex without the adamantyl functionalities was used, **3**·Eu^{3+}, no sensitization of the Eu^{3+} luminescence was observed. This control experiment shows that direct coordination of the carboxylate is too weak to immobilize **3**·Eu^{3+} on surface-bound **2** and has to be assisted by anchoring of both ligands on the receptor surface to have the high effective concentration[2,3] promote the direct coordination, leading to efficient energy transfer (see also Supporting Information).

Local emission spectra were recorded to further characterize the patterned surface of **1**·Eu^{3+} and **2** (Figure 2b). The emission spectra were selectively collected from both the patterned and nonpatterned areas upon excitation in the UV (step $\mathbf{i}_b$). From the nonpatterned areas, the observed Eu^{3+} emission is faint and can be attributed to inefficient direct UV excitation of **1**·Eu^{3+} alone. However, a significantly higher intensity of Eu^{3+} emission is observed in the **1**·Eu^{3+}**/2** patterned area. Clearly the emission of Eu^{3+} is amplified in the area where energy transfer occurred between the naphthalene antenna and the lanthanide complex. Considering also the fact that twice as much **1**·Eu^{3+} is expected to be present in the nonpatterned area with respect to the printed areas, comparing the intensities at 614 nm, an amplification of a factor of 54 is found between the patterned and nonpatterned areas. To quantify the energy transfer efficiency between naphthalene and the lanthanide complexes, the naphthalene emission lifetimes were determined in the absence and presence of Eu^{3+} (see Supporting Information).

To study the stoichiometry of complexation between **2** and **1**·Eu^{3+}, a stepwise procedure (Scheme 1, method **ii**) was applied: μCP of solution mixtures of different molar ratios of **1** and **2** was used to generate patterns on the β-CD monolayer, with an empty β-CD monolayer as background for good image contrast and intensity assessment. Directly after printing (step $\mathbf{ii}_a$), the surface was imaged with fluorescence microscopy, followed by immersion in a $EuCl_3$ solution for 30 min (step $\mathbf{ii}_b$) and reimaging (Figure 3). The fluorescence intensities of the surface antenna and Eu^{3+} emission were plotted as a function of the molar fraction of antenna **2** (Figure 4). Since the printboard ensures that the total immobilized ligand concentration (**1** + **2**) remains constant, this plot fulfills the requirements for a Job plot. To our knowledge, this is the first

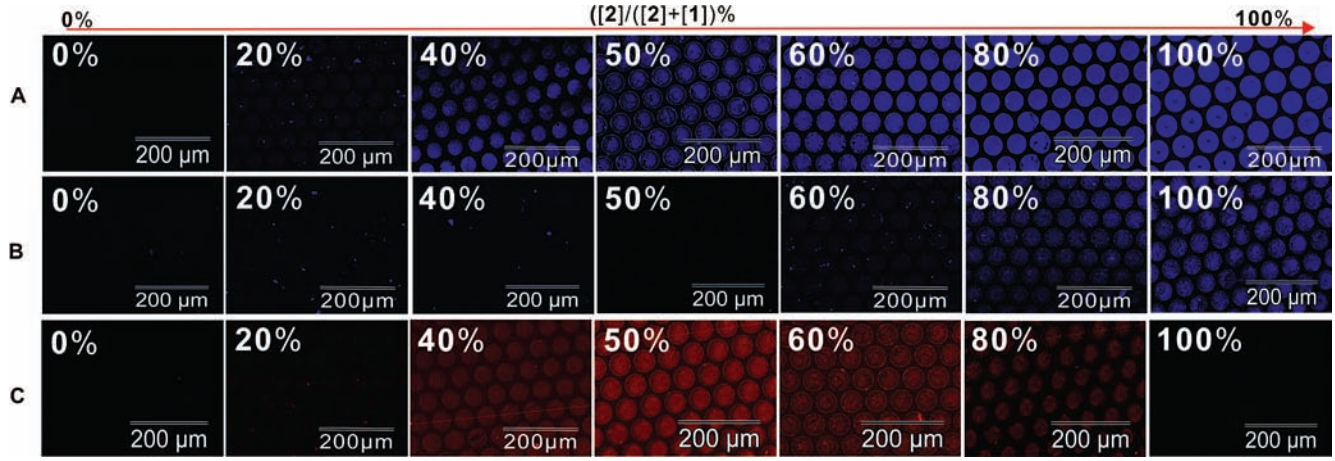

Figure 3. Fluorescence microscopy images of 50 μm dots prepared on β-CD monolayers by μCP (30 min) of solution mixtures of different ratios of **1** and **2** ($\mathbf{ii}_a$), followed by rinsing with Milli-Q water (A), and subsequently immersed in a solution of $EuCl_3$ for 30 min ($\mathbf{ii}_b$) (B, C), monitoring emission by the antenna (A, B; **B** filter) and by Eu^{3+} (C; **R** filter). The percentages of antenna **2** in the mixture of **1** and **2** are given in the images. The intensity profiles of all images are presented in the Supporting Information.

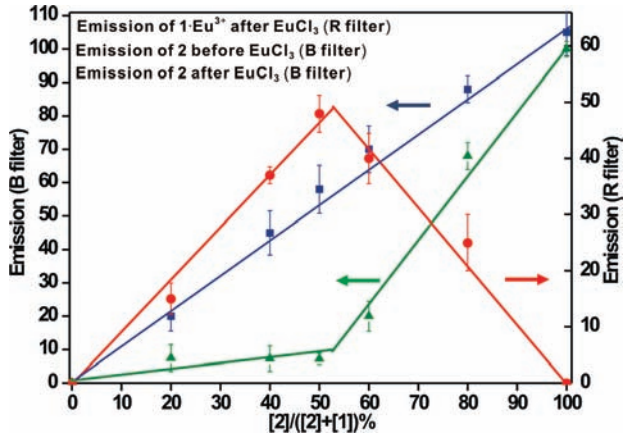

Figure 4. Fluorescence intensity of **2** before (blue, squares) and after (green, triangles) immersion in a $EuCl_3$ solution and of Eu^{3+} emission (red, circles) after the solution step, for patterns printed from solutions with varying ratios of **2** and **1**. Lines are presented for fits of the data points from 0−100% (blue line) and from 0−50% and 50−100% separately (green and red lines). The error bars represent a single standard deviation.

example of the use of a Job plot at a surface to study the stoichiometry of binding for a surface system.

The fluorescence intensity of the antenna before complexation with Eu^{3+} increases linearly with the antenna fraction (Figure 3A, Figure 4), confirming that the ratio of immobilized **1** and **2** is equal to the solution ratio used for printing. The images taken after immersion in the $EuCl_3$ solution show much lower antenna emissions (Figure 3B, filter **B**), particularly at fractions of antenna <50%, while strong Eu^{3+}emission (Figure 3C, filter **R**) is observed, which shows a maximum at an antenna fraction of 50% (Figure 4). These results show (i) quenching of antenna emission in accordance with energy transfer to the Eu^{3+} complex and (ii) optimal sensitized emission at a 1:1 antenna:Eu^{3+}-complex ratio, confirming the stoichiometry of the target complex (Figure 1b) to be 1:1. The sharpness of the inflection point in the Job plot indicates the complete formation of the target 1:1 complex. The apparently strong coordination of the carboxylate of **2** to the Eu^{3+} ion of **1**·Eu^{3+} is attributed to the high effective concentration at the surface[2,3] promoting the, now intramolecular, coordinative binding.

A thermodynamic model[15] was employed to simulate the surface Job plot data to check the validity of this method for verifying the stoichiometry of the complex of **1**·Eu^{3+}, **2** and the β-CD monolayer (see Supporting Information). The model can accurately reproduce the line trends observed in the Job plot and thus confirms the validity of the Job plot approach to assess the stoichiometry of a surface-assembled complex. The model also shows that the sharp break at a 1:1 ratio of **1**·Eu^{3+} and **2** can only be predicted if the binding constant is $>10^3$ M^{-1}. However, the absolute value of this stability constant is probably influenced by the dry state of the samples in which the fluorescence images were obtained.

This work clearly demonstrates that **1**·Eu^{3+} and the antenna **2** form a 1:1 coordination pair on the β-CD SAM. The formation of the target complex is directly indicated by the occurrence of sensitized luminescence. This surface assisted luminescence amplification has potential for developing optical devices or as a sensing platform for biologically relevant anions.[16] The system as a whole represents an example of functional expression, emerging from the combined system of all necessary components.[17] The high specificity of the complex formation is in part attributed to the multivalency of the receptor surface which is here translated in a higher-level multivalent interface of Eu complexes with vacant coordination sites and antenna molecules with the complementary carboxylate groups. Another crucial factor in steering the system into the direction of the target complex is to encode the necessary information into all individual building blocks. As can be seen here, this information can be limited while still complex molecular architectures can be achieved.

Acknowledgment. This work was supported by NanoNed, the nanotechnology program of the Dutch Ministry of Economic Affairs (Grant TMM 6976).

Supporting Information Available: Full experimental details including control experiments, lifetime measurements, synthetic procedures, other experimental procedures, and description of the thermodynamic modeling. This material is available free of charge via Internet at http://pubs.acs.org.

References

(1) (a) Reinhoudt, D. N.; Crego-Calama, M. *Science* **2002**, *295*, 2403–2407. (b) Campbell, V. E.; Nitschke, J. R. *Synlett* **2008**, *2008*, 3077–3090. (c) Bradley, J.; Holliday, C. A.M. *Angew. Chem., Int. Ed.* **2001**, *40*, 2022–2043. (d) Lehn, J.-M. *Chem. Soc. Rev* **2007**, *36*, 151–160. (e) Lehn, J.-M. *Proc. Natl. Acad. Sci. U.S.A.* **2002**, *99*, 4763–4768. (f) Whitesides, G. M.; Ismagilov, R. F. *Science* **1999**, *284*, 89–92. (g) Ludlow, R. F.; Otto, S. *Chem. Soc. Rev.* **2008**, *37*, 101–108. (h) Gibb, B. C. *Nat. Chem.* **2009**, *1*, 17–18.
(2) Langner, A.; Tait, S. L.; Lin, N.; Rajadurai, C.; Ruben, M.; Kern, K. *Proc. Natl. Acad. Sci. U.S.A.* **2007**, *104*, 17927–17930.
(3) Mulder, A.; Huskens, J.; Reinhoudt, D. N. *Org. Biomol. Chem.* **2004**, *2*, 3409–3424.
(4) Ludden, M. J. W.; Reinhoudt, D. N.; Huskens, J. *Chem. Soc. Rev.* **2006**, *35*, 1122–1134.
(5) Eigen, M. *The Hypercycle: A Principle of Natural Self Organization*; Springer-Verlag: 1979.
(6) (a) Crespo-Biel, O.; Lim, C. W.; Ravoo, B. J.; Reinhoudt, D. N.; Huskens, J. *J. Am. Chem. Soc.* **2006**, *128*, 17024–17032. (b) Ludden, M. J. W.; Mulder, A.; Schulze, K.; Subramaniam, V.; Tampe, R.; Huskens, J. *Chem.—Eur. J.* **2008**, *14*, 2044–2051.
(7) Lim, C. W.; Crespo-Biel, O.; Stuart, M. C. A.; Reinhoudt, D. N.; Huskens, J.; Ravoo, B. J. *Proc. Natl. Acad. Sci. U.S.A.* **2007**, *104*, 6986–6991.
(8) Hazenkamp, M. F.; Blasse, G.; Sabbatini, N. *J. Phys. Chem.* **1991**, *95*, 783–787.
(9) Buonocore, G. E.; Li, H.; Marciniak, B. *Coord. Chem. Rev.* **1990**, *99*, 55–87.
(10) Dexter, D. L. *J. Chem. Phys.* **1953**, *21*, 836–850.
(11) Michels, J. J.; Huskens, J.; Reinhoudt, D. N. *J. Am. Chem. Soc.* **2002**, *124*, 2056–2064.
(12) Delgado-Pinar, E.; Frias, J. C.; Jimenez-Borreguero, L. J.; Albelda, M. T.; Alarcon, J.; Garcia-Espana, E. *Chem. Commun.* **2007**, 3392–3394.
(13) (a) Massue, J.; Quinn, S. J.; Gunnlaugsson, T. *J. Am. Chem. Soc.* **2008**, *130*, 6900–6901. (b) Ai, K. L.; Zhang, B. H.; Lu, L. H. *Angew. Chem., Int. Ed.* **2009**, *48*, 304–308. (c) Ipe, B. I.; Yoosaf, K.; Thomas, K. G. *J. Am. Chem. Soc.* **2006**, *128*, 1907–1913.
(14) The surface was consecutively imaged by fluorescence microscopy using two different filter sets: one set allows UV excitation and red emission using a narrow bandpass filter centered at 610 nm (**R**, which only collects the emission of Eu^{3+}), and another set allows UV excitation and blue emission (**B**, which only collects the emission of the naphthalene moiety).
(15) Huskens, J.; Mulder, A.; Auletta, T.; Nijhuis, C. A.; Ludden, M. J. W.; Reinhoudt, D. N. *J. Am. Chem. Soc.* **2004**, *126*, 6784–6797.
(16) Leonard, J. P.; dos Santos, C. M. G.; Plush, S. E.; McCabe, T.; Gunnlaugsson, T. *Chem. Commun.* **2007**, 129–131.
(17) Luisi, P. *Fundam. Chem.* **2002**, *4*, 1572–8463.

JA904747P